Instrumented Static Pile Load Testing of Cast-in-place Concrete Piles in Edmonton

Evan Sau Yue Ma, Michan Condra, and Andrew Cushing
Arup Canada Inc., Toronto, Ontario, Canada

Michael Lewis
Bechtel Infrastructure, Evans, Georgia, USA

ABSTRACT
Cast-in-place concrete piles were used to support transportation structure foundations for the Valley Line Light Rail Transit project in Edmonton. A series of instrumented conventional static, Osterberg Load Cell (O-Cell) sacrificial pile load tests, and Statnamic (rapid) proof load tests were used to confirm shaft friction and end bearing parameters used in design at three sites along the alignment. This paper evaluates the pile capacities derived from common empirical analysis (α and β-methods) from laboratory and field testing with the results of the sacrificial load tests. Further, the mobilized unit skin friction and end bearing values are compared with established empirical skin-friction settlement (t-z), and end bearing-toe settlement (q-w) curves respectively. Proof load testing is assessed against the static top load and equivalent top load from O-Cell testing plotted with normalized settlement/diameter ratios.

RESUME
Les fondations de certaines structures de transport du projet de train léger sur rail Valley Line à Edmonton consistent de pieux forés. Une série de différents types d'essais de charge sur pieux sacrificiels a été complétée, dont des essais statiques conventionnels de charge sacrificielle statique, Osterberg Load Cell (O-Cell), et des tests de charge étalon (rapide) statnamiques. mlbCes essais ont servi à confirmer les paramètres de résistance de pointe et de frottement latéral utilisés dans la conception sur trois sites le long de l'alignement. Cet article évalue les capacités portantes dérivées d'analyses empiriques communes (méthodes α et β) à partir d'essais en laboratoire et sur le terrain avec les résultats des essais de charge sacrificiels. En outre, les valeurs mobilisées de frottement latéral et de résistance de pointe sont comparées aux courbes empiriques établies de charge-déplacement du fût (t-z) et de la pointe (q-w) respectivement. Les essais de charge sont évalués par rapport à la charge statique supérieure et à la charge supérieure équivalente des tests O-Cell tracés avec des rapports normalisés de tassement / diamètre.

1 INTRODUCTION

The Valley Line LRT is a new 13 km long Light Rail Transit (LRT) Line currently under construction in the City of Edmonton, Alberta, Canada. The line starts in downtown Edmonton, crosses the North Saskatchewan River, and heads due south to the Mill Woods area. The project is a Public-Private Partnership (P3) between the City of Edmonton and TransEd LRT Partners, comprised of Bechtel Canada, EllisDon, Bombardier, and Fengate Capital. This paper will focus on piled foundations at three sites of the project, shown in Figure 1:

- Operations & Maintenance Facility (OMF)
- South River Valley (SRV) Elevated Guideway
- Davies Station & Elevated Guideway

The OMF and the Elevated Guideway Structures are to be founded on bored pile (drilled shaft) foundations up to 2.5 m diameter, installed through surficial overburden soils and socketed into the underlying clay shale unit. A full-scale load testing program was undertaken on sacrificial piles, in addition to proof testing of production piles. Load testing techniques employed on this project include conventional load frame (top load) compression testing, Osterberg cell (O-Cell) testing, and Statnamic (rapid) proof-load testing of production piles.

2 SCOPE AND BACKGROUND

The scope of this paper presents the unit skin friction and end bearing resistances obtained from instrumented pile load testing. These values are evaluated with common empirical methods used for pile design, and normalized load transfer-settlement curves (Reese and O'Neil, 1987). Load deflection behavior between equivalent top down static and Statnamic pile load testing are also compared.

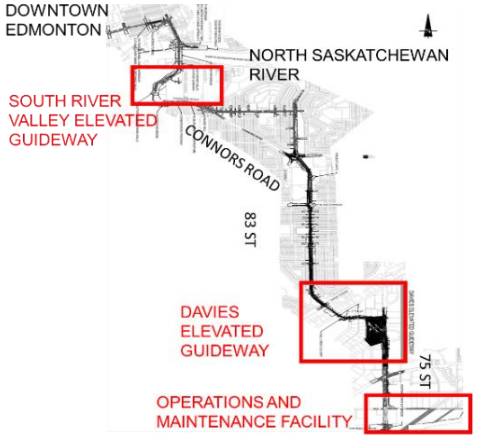

Figure 1. Key plan of Valley Line LRT Alignment showing the three sites of focus

2.1 Subsurface Stratigraphy and Investigation

The geology in Edmonton typically consists of glacio-lacustrine sediments (post-glacial) overlying stiff, heavily jointed glacial tills. Intra-till sand pockets (Matheson, 1970) are commonly found within the till. The glacial till is underlain by bedrock consisting of the Cretaceous Horseshoe Canyon Formation Shales of the Edmonton Group.

Auger drilling was completed within 10 m of pile load tests to confirm stratigraphy. Index testing, including natural moisture content (w_n), plasticity index (PI), fines content (FC), Rock Quality designation (RQD), and Standard Penetration Test (SPT), was supplemented with field vane testing, and laboratory testing consisting of Consolidated Isotropically Undrained (CIUC), Unconsolidated Undrained (UU), triaxial, and 1D incrementally loaded oedometer tests. Figure 2 shows the undrained shear strength at the Davies Elevated Guideway site from laboratory testing and field data.

2.1.1 Operation and Maintenance Facility (OMF)

Two conventional static load tests were performed on piles constructed in 1m of clay fill, overlying 1.5 to 2.5 m of firm glacio-lacustrine clay (w_n=25%±5% [mean±SD], PI=31±7%, overconsolidation ratio, OCR=5-8), and up to 7 m of glacial clay till (w_n=22±5%, PI=26±9%, OCR=2-5), and finally terminating in weak clay shale bedrock at depths of 3.5 and 9.5 m (w_n=24±3%, PI=47±11%, RQD=80±20%).

2.1.2 South River Valley (SRV) Elevated Guideway

A single O-Cell test was performed on a pile drilled into 1m of clay fill, overlying 7 m of loose sand (w_n=13±6%, FC=53±26%), and 3 m of dense fluvial terrace gravel (w_n=10±5%, FC=10%) deposits and terminating in clay shale (w_n=18±5%, PI=91%, RQD=45±32% above a depth of 17 m, RQD=77±24% below a depth of 17 m).

2.1.3 Davies Elevated Guideway

Two O-Cell tests were conducted in 5 m of glacial-lacustrine (w_n=26±4%, PI=34±3%, OCR=4.5) clay, overlying 9 to 19 m of glacial clay till (w_n=19±4%, PI=22±7%, OCR=1.5-3.0), intra-till sands (w_n=19±5%, FC=35±26%) and bearing in weak clay shale bedrock (w_n=24±5%, RQD=66±33% above a depth of 25 m, RQD=81±17% below a depth of 25m), interbedded with sandstone (w_n=22±2%, RQD=85±15% above a depth of 25 m, RQD=95±6% below a depth of 25 m).

2.2 Empirical Side Resistance

A common method of estimating the ultimate unit side resistance (q_s) of piles and shafts in clay soils under undrained conditions is the Alpha (α) Method, in which:

$$q_s = \alpha\, s_u \quad [1]$$

where,

s_u = undrained soil shear strength

α = adhesion factor ≤ 1.0

Relationships between α and s_u have been proposed (eg. $\alpha=0.21+0.26\ p_a/s_u$ by Stas and Kulhawy, 1984). The Beta method (β) method under drained conditions is as follows:

$$q_s = \beta\ \sigma'_v = K_s \tan\delta'\ \sigma'_v \quad \text{where,} \quad [2]$$

σ'_v = vertical effective soil stress

δ' = effective pile wall-soil interface friction angle

K_s =coefficient of lateral earth pressure, which is typically considered to be equal to coefficient of earth pressure at rest, K_0.

Side resistance in rock is often correlated with the Unconfined Compressive Strength (UCS) of the rock and an empirical factor, b.

$$q_s/p_a = b(UCS/p_a)^{0.5} \quad [3]$$

where,

p_a = atmospheric pressure

A wide range of empirical factors (b=0.63 to 1.41) have been proposed by Rowe and Armitage (1984), Horvath et al.(1983), and Carter and Kulhawy (1988).

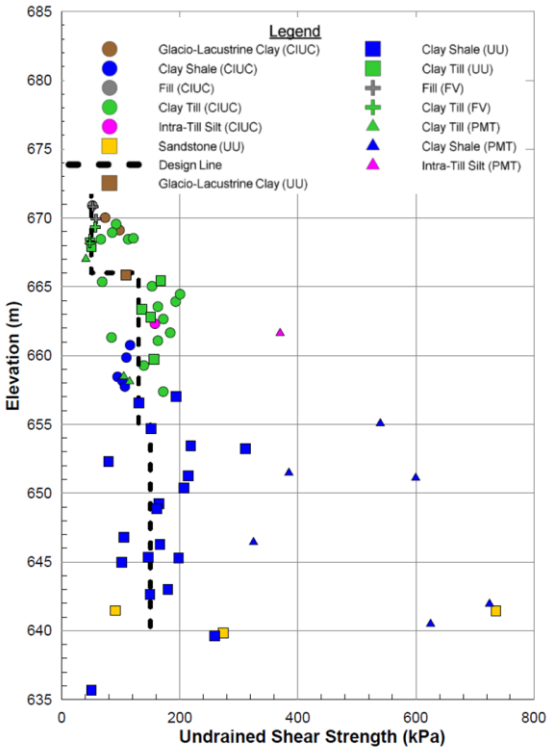

Figure 2. Undrained shear strength at Davies Elevated Guideway from various field and laboratory tests.

2.3 Empirical End Bearing Resistance

The ultimate end bearing resistance (q_t) in clay soils using undrained analysis can be expressed as a function of undrained shear strength (s_u) as follows:

$$q_t = N_t\, s_u \quad [4]$$

N_t = bearing capacity factor in clay

CFEM (2006) suggests a range of N_t of 6 to 9, varying as a function of pile diameter. Similar expressions for weak rock have been proposed:

q_t = 2.5 UCS (Rowe and Armitage, 1987) [5a]
q_t = 5.0 UCS (Williams et al., 1980) [5b]
q_t = 3 K_{sp} d UCS (Ladanyi and Roy, 1971) where, [5c]
K_{sp} = empirical factor for fracture spacing, varying between 0.1 and 0.4
d = 1+0.4 L_s/B_s [6]
L_s= Length of socket
B_s= Diameter of socket

2.4 Historical Tests

Several published load tests have been conducted in the Edmonton area. Thomson (1981) evaluated the results of conventional top load compression testing conducted at seven sites. The study suggests values of α=0.45 and a N_t=9 for the clay soils in the surrounding region. More recently, Osterberg O-Cell load tests instrumented with strain gauges were conducted, including at the Anthony Henday Drive South East Ring Road (AHDSERR), North-West Anthony Henday Drive (NWAHD), and the ICE District Towers. The results of these test results have been summarized in Table 1.

Table 1. Mobilized Side Resistance and End Bearing of Bored Piles from Osterberg O-Cell load testing

Location	*Material*	*Skin Friction (kPa)*	*End Bearing (kPa)*	*Reference*
AHDSERR (17th Street)	Clay Till	27-77	895	Skinner et al. (2008)
AHDSERR (Hwy 14 Ramps)	Clay Till	44-102	-	
	Bentonite/ Clay Shale	58	2028	
AHDSERR (34th Avenue)	Clay Till	35-104	1300	
NWAHD (127 Street)	Clay	41-60	-	Ruban and Kort (2011)
	Clay Till	55-119	1287	
NWAHD (127 Street)	Clay	40-48	-	
	Clay Till	82	-	
	Clay Shale	95-116	6041	
ICE District Towers (Test 1)	Clay Till	96	-	Wang et al. (2017)
	Empress Sand	183-199	-	
	Clay Shale	129-297	7022	
ICE District Towers (Test 2)	Empress Sand	269	-	
	Clay Shale	99-566	11385	

3 RESULTS

3.1 Extrapolation of Load to Failure

For large diameter bored piles in rock, it can be impractical to load a pile to failure as large movements are required to mobilize ultimate resistance, either exceeding the practical movements for a sacrificial test or by exceeding the limits of the Osterberg load cell. Hirany and Kulhawy (1989) suggest an interpretation of failure load as the load mobilized at pile head movement of 4% of shaft diameter. Similarly, Reese and O'Neill (1987) estimate maximum unit skin friction to be mobilized at a movement of 0.8% shaft diameter and maximum end bearing to be mobilized at a movement of 10% shaft diameter. For this paper, the Chin (1970) and Decourt (1999) hyperbolic extrapolation methods were used to extrapolate the unit skin friction resistance to 0.8% shaft diameter, and unit end bearing resistance to 10% shaft diameter, where ultimate resistance was not reached. The interpolated and extrapolated values are presented alongside the mobilized values from pile load testing.

3.2 OMF Static Pile Load Test

OMF Test Pile 1 (TP1) was a 1000 mm diameter pile installed to a depth of 10.4 m in an unsupported hole in dry conditions. Four 508 mm diameter piles belled at 1000 mm were used for reaction. Test Pile 2 (TP2) was a 600 mm diameter pile installed to a depth of 16m using a temporary casing, which resulted in a dry pile bore. Four 508 mm diameter piles belled at 750 mm were used for reaction. Both test piles were instrumented with eight pairs of concrete embedment strain gauges and eight pairs of sister bar strain meters, and four crosshole sonic logging (CSL) tubes. Pile head movement was monitored with two linear variable displacement transducers (LVDTs) and two dial gauges mounted on a steel plate at the pile head. Two telltales were installed on the rebar cage at each pile to measure movements at the base using two linear potentiometers. The test load was applied with a 9800 kN calibrated hydraulic jack, in accordance with ASTM D1143 Quick Test Method. The mobilized unit skin friction and end bearing results are summarized in Table 2 and Table 3 for TP1 and TP2, respectively. Some levels of strain gauges were ignored in the analysis to achieve a sensible interpretation.

Table 2. OMF TP-1– Test Pile Stratigraphy and Mobilized Skin Friction and End Bearing Values

Strain Gauge Depth (m)	*Stratigraphy*	*Average*		*Skin Friction (kPa)* †	
		SPT (N)	*s_u (kPa)*	*Max Mob.*	*Mobilized @ 0.8% Pile Diameter*
1-3.5	Clay	8	40	29	27
3.5-5.5	Clay Shale	28	500	92	53
5.5-7.5	Clay Shale	-	450	61	54
7.5-9.5	Clay Shale	-	450	45	41
		Design		End Bearing (kPa)	
		SPT (N)	*s_u (kPa)*	*Mob.*	*Extrapolated*
10	Clay Shale	-	450	1126	1200

†Interpolated to a movement of 0.8% shaft diameter

Table 3. OMF TP-2 – Test Pile Stratigraphy and Mobilized Skin Friction and End Bearing Values

Strain Gauge Depth (m)	*Stratigraphy*	*Average*		*Skin Friction (kPa) †*	
		SPT (N)	*s_u (kPa)*	*Max Mob.*	*Mobilized @ 0.8% Pile Diameter*
1.0-4.0	Clay/Clay Till	8	55	24	24
4.0-9.5	Clay Till	18	90	53	36
9.5-10.5	Clay Shale	23	450	149	126
10.5-12.0	Clay Shale	25	450	63	54
12.0-13.0	Clay Shale	-	400	174	120
13.0-15.5	Clay Shale	-	350	122	108
		Design		End Bearing (kPa)	
		SPT (N)	*s_u (kPa)*	*Mob.*	*Extrapolated*
16	Clay Shale	-	350	1337	1360

†Interpolated to a movement of 0.8% shaft diameter

3.3 SRV Elevated Guideway – Osterberg Load Cell

SRV Test Pile 3 (STP3) was a 1800 mm diameter pile installed to a depth of 21.6 m. The pile bore was drilled using a 13 m temporary casing, though the pile was ultimately poured in wet conditions. One 610 mm diameter O-Cell was located 670 mm above the pile tip. The pile was instrumented with eight levels of two pairs of sister bar vibrating wire strain gauges, four linear vibrating wire displacement transducer (LVWDTs) positioned at the upper and lower plates of the O-Cell assembly, four CSL tubes, and four telltales to the top of the O-Cell.

Table 4. SRV Elevated Guideway STP-3 (Pier 4) – Test Pile Stratigraphy and Mobilized Skin Friction and End Bearing Values

Strain Gauge Depth (m)	*Stratigraphy*	*Design*		*Skin Friction (kPa)**	
		SPT (N)	*s_u (kPa)*	*Mobilized*	*Extrapolated*
0-3.2	Loose Silty Sand	5	-	15	19
3.2-6.7	Loose Silty Sand	5	-	27	29
6.7-7.7	Gravel	40	-	131	178
7.7-10.4	Gravel	38	-	74	89
10.4-15.9	Clay Shale-Coal	45	300	227	287
15.9-20.5	Coal-Clay Shale-Sandstone	-	-	41	-
		Design		End Bearing (kPa)*	
		SPT (N)	*s_u (kPa)*	*Mobilized*	*Extrapolated*
20.5	Clay Shale		1150	4729	4978

* Mobilized values as reported by LOADTEST (2017c)

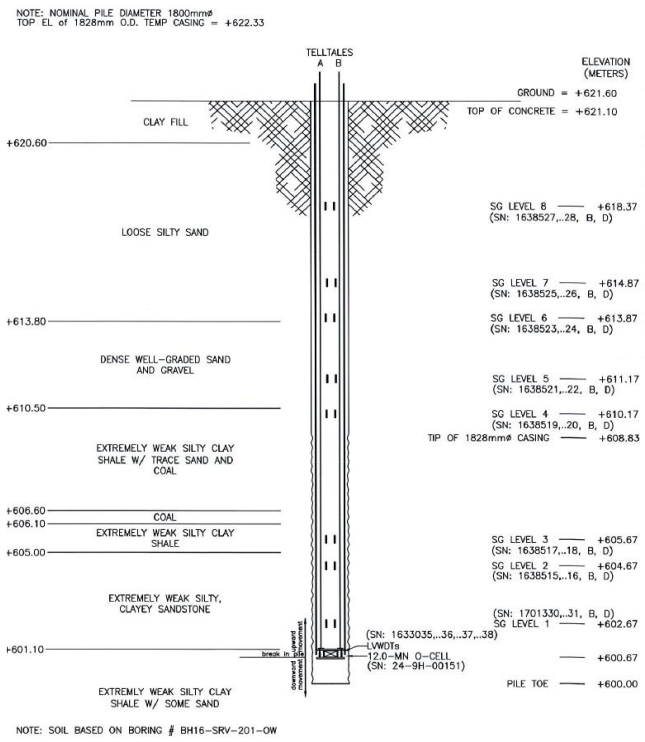

Figure 3. Test Pile Instrumentation at SRV (LOADTEST, 2017c)

The load test was conducted in accordance with ASTM D1143 Quick Test Method, with each successive load increment held for eight minutes to a bi-directional load of 12.2 MN. The unit skin friction and end bearing results are summarized in Table 4. Figure 3 shows the stratigraphy and locations of O-Cell and strain gauges at the SRV site.

3.4 Davies Elevated Guideway – Osterberg Load Cell

Davies Test Pile 1 (STP1) was a 1800 mm diameter pile installed to a depth of 35.0 m with a 10 m temporary casing. One 610 mm diameter O-Cell was located 5.6 m above the pile tip. Test Pile 2 (STP2) was a 2500 mm diameter pile installed to a depth of 35.0 m, drilled with the support of polymer slurry and a 5m temporary casing. One 660 mm diameter O-Cell was located 2.9m above the pile tip. The piles were instrumented with eight levels of two pairs of sister bar vibrating wire strain gauges, four LVWDTs positioned at the upper and lower plates of the O-Cell assembly, four embedded compression telltales (ECTs) positioned below the O-Cell, four CSL tubes, and four telltales to the top of the O-Cell The load test was conducted in accordance with ASTM D1143 Quick Test Method, with each successive load increment held for eight minutes to a bi-direction load of 20.6 MN for TP1, and 17.3 MN for TP2. The unit skin friction and end bearing results are summarized in Table 5 and Table 6 for STP1 and STP2 respectively.

It should be noted that for the STP2 strain gauges at depths of 3.6-9.6 m, and 11.6-19.6 m, very low skin frictions were mobilized, and a hyperbolic extrapolation

could not be credibly interpreted. It is unlikely that the unit skin friction values were ultimate values, due to the small displacements mobilized during the test. Therefore, these results are presented, but were not included in subsequent analysis.

Table 5. Davies Elevated Guideway STP-1 (Pier 15) – Test Pile Stratigraphy and Mobilized Skin Friction and End Bearing Values

Strain Gauge Depth (m)	*Stratigraphy*	*Design*		*Skin Friction (kPa)**	
		SPT (N)	*s_u (kPa)*	*Mobilized*	*Extrapolated*
0-4.1	Clay	7	50	27	31
4.1-7.1	Clay	22	100	47	51
7.1-9.6	Clay Till	17	150	95	112
9.6-12.1	Clay Till	29	150	161	189
12.1-18.1	Clay Shale	29	170	146	184
18.1-28.1	Clay Shale	-	170	158	186
28.1-32.6	Sandstone-Clay Shale	-	370	313	180†
		Design		End Bearing (kPa)*	
		SPT (N)	*s_u (kPa)*	*Mobilized*	*Extrapolated*
33.7	Sandstone-Clay Shale		370	4195	5344

* Mobilized values as reported by LOADTEST (2017a)
†Interpolated to a movement of 0.8% shaft diameter

Table 6. Davies Elevated Guideway STP-2 (Pier 25) – Test Pile Stratigraphy and Mobilized Skin Friction and End Bearing Values

Strain Gauge Depth (m)	*Stratigraphy*	*Design*		*Skin Friction (kPa)**	
		SPT (N)	*s_u (kPa)*	*Mobilized*	*Extrapolated*
3.6-9.6	Clay	13	50	15	-
9.6-11.6	Silty Sand	24	-	67	-
11.6-19.6	Clay Till	18	95	17	-
19.6-23.6	ClayTill / Silty Sand	36	95	68	107
23.6-29.6	Clay Shale-Sandstone	34	330	155	180
29.6-32.1	Clay Shale	-	240	128	-
34.1-35.0	Clay Shale	-	240	520	450†
		Design		End Bearing (kPa)*	
		SPT (N)	*s_u (kPa)*	*Mobilized*	*Extrapolated*
35	Clay Shale / Coal		240	1137	2116

*Mobilized values as reported by LOADTEST (2017b)
†Interpolated to a movement of 0.8% shaft diameter

4 DISCUSSION

4.1 Evaluation of Empirical Pile Design Approaches

4.1.1 α-Method Skin Friction

The α-values were back-calculated from the larger of the maximum mobilized or the extrapolated skin friction at 0.8% pile diameter from the pile load test results and the best-estimate s_u. These values were then compared with the predicted α-values using the α-s_u relationship proposed by Stas and Kulhawy (1984) and Weltman and Healy (1976) for glacial tills. The results are plotted in Figure 4.

There is considerable scatter in the back-calculated α-values. Average back-calculated α-values for glacio-lacustrine clay was 0.57±0.13, while the empirical predictions vary from 0.47 to 0.87 for the range of undrained shear strengths. The average back-calculated α-values for the clay till was 0.93±0.31. Predicted α-values range from 0.39 to 0.83 from the empirical models. The average back-calculated α-values in clay shale was 0.63±0.61, with the predicted values range from 0.26 to 0.36. This indicates a poor relationship overall, and the average skin resistance is under-predicted in the clay till and clay shale by empirical methods.

4.1.2 β-Method skin friction

β-values were back-calculated from an estimation of the effective stress for the silty sand, loose silty sand and the gravels at the three sites. Average β-values 0.56±0.32 ranged from 0.28 to 1.18. Using a typical friction angle correlations from SPT (Hatanaka and Uchida, 1996), and assuming $K_s/K_0=1$ for bored piles, the K_0 was estimated to range from 0.41 to 1.18, generally decreasing with depth.

4.1.3 Empirical Factors in Rock

For the calculation of skin friction in clay shale, empirical factor, b from Equation 3, was back-calculated from the best-estimate UCS (taken as two times the s_u). Average b parameter was calculated to be 0.64±0.57. While the average value is within the range shown by Horvath et al (1983) for limits states design, there is considerable scatter in the data. Empirical factor, b, was back-calculated to be 0.66 and 0.70 for the interbedded clay shale and sandstone.

For end-bearing, N_t was back-calculated based on the extrapolated values at 10% pile diameter movement. Four tests terminated in clay shale, and one test was terminated in an interbedded layer of sandstone and clay shale. Average N_t for the piles terminated in the clay shale only was 5.85±2.03. This value is slightly lower than the range provided in the CFEM (2006), though it is consistent with relationship for weak rock proposed by Rowe and Armitage (1987). It should be noted that N_t was calculated to be 14.4 for the test in interbedded sandstone and clay shale.

4.1.4 Uncertainty

Although the subsurface conditions were known relatively well, there is still uncertainty, particularly in the intermediate soil materials. Sand and silt lenses in the clay till may result in partially drained behavior, as opposed to idealized undrained-α pile behaviour. This coupled with the different construction techniques used (e.g., dry auger

drilling and polymer slurry stabilization), also contributed to the scatter in the results.

4.2 Comparison with Normalized Load Transfer Settlement Curves

Axial load-settlement behavior of a pile is often modelled in numerical analysis by the t-z curve method. Non-linear soil behavior is modelled as a series of springs at the pile-soil interface with skin friction-settlement (t-z) curves. End bearing is simulated with similar non-linear end bearing-pile tip movement (q-w) curves. The results of the pile load test were normalized and plotted with the upper and lower bound empirical curves proposed by Reese and O'Neill (1987) and that are used in programs such as Ensoft GROUP/SHAFT. The mobilized skin friction resistance was normalized by the larger of the maximum mobilized or the extrapolated unit skin friction at 0.8% pile diameter. The mobilized end bearing resistance was normalized by the extrapolated end bearing at 10% pile diameter. The abscissa was normalized by pile diameter. Figure 5 through Figure 7 show the normalized load-deflection behavior of the test piles.

In general, there is good agreement between the soil t-z curves and the upper and lower bound empirical curve, particularly in the initial "elastic" portion of the curves. However, notably, the clay till showed a softer response in the elastic range, and exhibited strain hardening beyond 0.8% pile diameters, with a peak value not mobilized until at least movement equal to 2% shaft diameter.

There is less of an agreement between the upper and lower bound curves and the bedrock, and greater variety of load deflection behavior. Four of the unit skin friction curves in Figure 6 show a softer response in the elastic range and strain-hardening behavior. Three other curves showed a stiffer behavior than is predicted by the empirical model in the elastic range and post-peak strain softening behavior. Peak unit skin friction was mobilized from a range of 0.1% to >2% pile diameter movement.

The unit end bearing movement curves show that for the piles terminating in clay shale, the pile tests show slightly less stiff behavior than is predicted by the empirical model. For the single pile test terminating in interbedded clay shale and sand stone, a stiff load-deflection behavior was observed. A peak ultimate unit end bearing was not observed in the available testing.

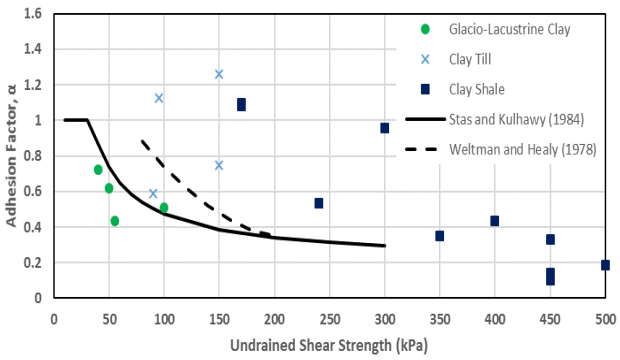

Figure 4. Back-calculated alpha values from pile load test compared against a typical empirical relationship.

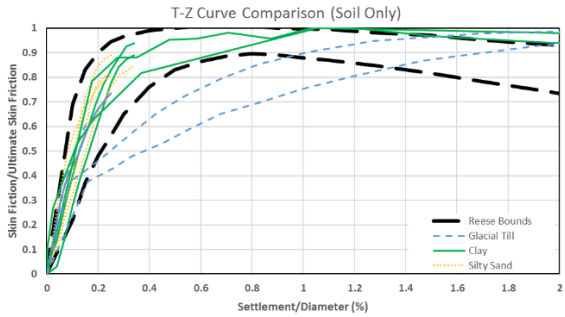

Figure 5. Normalized skin friction in soil from pile load test

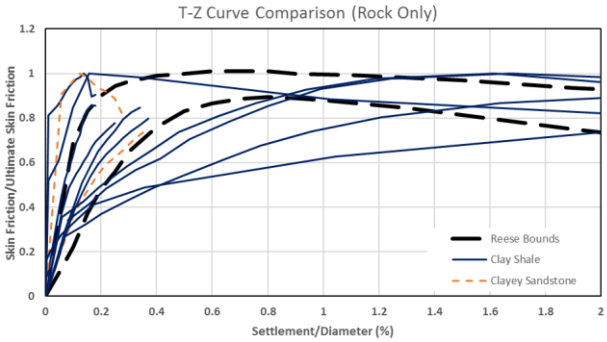

Figure 6. Normalized skin friction in rock from pile load test

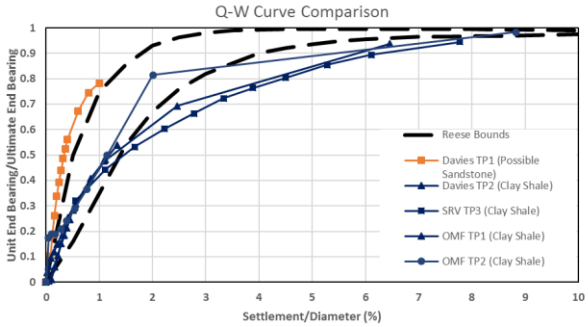

Figure 7. Normalized end bearing in rock from pile load tests.

4.3 Load Deflection Behavior of Static and Statnamic Pile Load Tests

A series of Statnamic rapid proof load tests were completed at SRV and Davies in general accordance with the ASTM D7383-10, and tested to 1.0 times the factored axial load demand. These were completed at the following piles:

- SRV Pier 7 (1800 mm diameter)
- Davies Pier 10 (1800 mm diameter)
- Davies Pier 18 (2500 mm diameter)

The analysis of the Statnamic load test data was completed by AFT (2017 a, b, c) using the Modified Unloading Point method and equivalent top-load-displacement curves. These curves were plotted against the equivalent top-load-displacement curves produced by LOADTEST (2017 a, b,

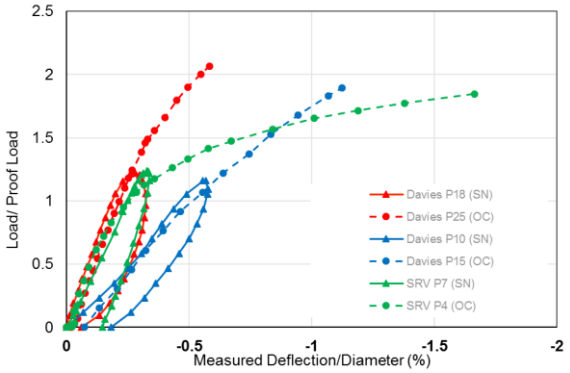

Figure 8. Equivalent top load of Statnamic and Osterberg load test normalized by proof load and pile diameter

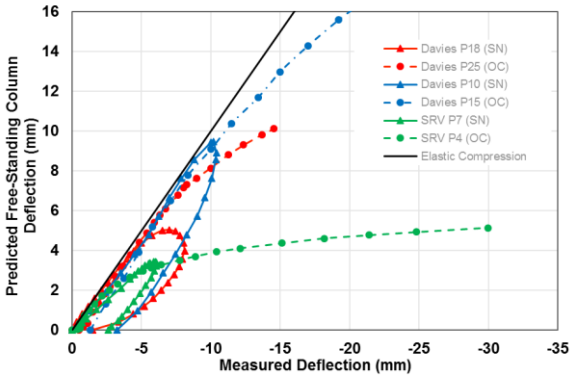

Figure 9. Measured deflections plotted against elastic compression of a free-standing column

c). The load in both curves were normalized by the proof load, and the abscissa was normalized by pile diameter, shown in Figure 8. In addition, the measured displacements were plotted against the theoretical displacement of a free-standing column displacement (elastic compression) of the pile in Figure 9.

As shown in the Figure 8, the equivalent top load-displacement curves produced for the Statnamic test, plot closely up to the factored proof load with the equivalent top load-displacement curves at the nearest Osterberg Cell test location. This shows that the methods used to construct the curves produce consistent load-deflection behavior. In both cases, the test results show that the piles behave elastically at working loads, which is consistent with general practice.

Figure 9 shows the departure of the load-deflection behavior from pure elastic compression of the concrete pile. The idealized compression of a free-standing column is used widely for the estimation of failure load, such as in the Davisson (1970) Offset Limit Load method. Displacement outside of elastic compression of the pile was observed from approximately 3 to 6 mm, equivalent to 0.2% to 0.3% of the pile diameter.

5 CONCLUSION

Several pile tests were performed on foundations for the Edmonton Valley Line project, including conventional axial load tests, O-Cell tests, and Statnamic proof tests. The test results show a considerable amount of variability in mobilized skin friction resistance between piles as well as along each pile, even in the same stratigraphic unit. This may be due to inherent uncertainty in the subsurface conditions and the different installation techniques used for installation. It was shown in a back analysis that both the α-methods for determining side resistance, and empirical methods for rock, presented in typical design guidance such as the CFEM (2006), were poor predictors for mobilised resistance. The alpha method may not be suitable for intermediate materials such as clay till and clay shale. Therefore, the Authors believe it is prudent that drained methods such as the beta method should also be used concurrently with the alpha method to design bored piles in these materials.

The measured load-deformation curves in clay and sands generally showed good agreement with the bounds of the t-z and q-w empirical curves proposed by Reese and O'Neill (1987), particularly in the elastic deformation regime. However, the clay till and shales results plotted outside these bounds. These results from the sacrificial static load testing program underline the requirement and benefits of performing pile testing programmes to confirm pile design parameters and spring stiffness values used for geo-structural design.

Finally, the equivalent top load-displacement curves produced for the Statnamic proof tests were in good agreement with the equivalent top load-displacement curves produced for nearby O-Cell tests. At least in the context of this project, Statnamic tests appeared to be a useful tool to supplement O-Cell tests for testing of large diameter piles.

6 ACKNOWLEDGEMENTS

The authors are grateful to the City of Edmonton, the owner and sponsor of the project, and TransEd, the design-build contractor and 30-year operator and maintainer of the project, for the support and permission for the publication of this paper. We are also grateful to LOADTEST, Inc. for their support of the O-cell testing, AFT for the Statnamic testing, and foundation subcontractors AGRA, Keller, and Doublestar Drilling for test and production pile drilling.

7 REFERENCES

AFT (2017a). *Final Report of Axial STATNAMIC Load Testing – Production Shaft P7-2 at South River Valley* (SRV), Edmonton Valley Line LRT Stage 1; August 25, 2017, Advanced Foundation Testing, Green Cove Springs, Florida.

AFT (2017b). *Final Report of Axial STATNAMIC Load Testing – Production Shaft P10-1 at Davies Elevated Guideways*, Edmonton Valley Line LRT Stage 1; August 14, 2017, Advanced Foundation Testing, Green Cove Springs, Florida.

AFT (2017c). *Final Report of Axial STATNAMIC Load Testing – Production Shaft P18-A-1 at Davies Elevated Guideways*, Edmonton Valley Line LRT Stage 1;

August 14, 2017, Advanced Foundation Testing, Green Cove Springs, Florida.

ASTM D1143/D1143M-07, *Standard Test Methods for Deep Foundations Under Static Axial Compressive Load*

ASTM D7383-10, *Standard Test Methods for Axial Compressive Force Pulse (Rapid) Testing of Deep Foundations*

Carter, J.P. and Kulhawy, F.H. (1988). Analysis and Design of Drilled Shaft Foundations Socketed into Rock. *Report EI-5918*, Electric Power Research Institute, Palo Alto, Calif.

Chin, F.K. (1970). Estimation of the Ultimate Load of Piles not carried to Failure. Proceedings, *2nd Southeast Asian Conference on Soil Engineering*, Singapore, pp. 81-90.

CFEM (2006). *Canadian Foundation Engineering Manual, Fourth Edition*, Canadian Geotechnical Society.

Davisson, M.T. (1970). Lateral Load Capacity of Piles. Highway Research Board, Washington, D.C., *Highway Research Record No. 333*, pp. 104-112.

Decourt, L. (1999). Behavior of foundations under working load conditions. Proceedings of the *11th Pan American Conference on Soil Mechanics and Geotechnical Engineering*, Foz Dulguassu, Brazil, Vol: 04, pp. 453-488.

Hatanaka, M. and Uchida, A. (1996). Empirical Correlations Between Penetration Resistance and Internal Friction Angle of Sandy Soils: *Soils and Foundations.* Japanese Geotechnical Society Vol: 36, No. 4, 1-9

Hirany, A. and Kulhawy, F.H. (1989). Interpretation of Load Tests on Drilled Shafts (1): Axial Compression. Foundation Engineering: *Current Principles and Practices (GSP 22),* ASCE, New York, pp. 1132-1149.

Horvath R.G., Kenney, T.C. and Kosicki, P. (1983). Method of lmproving the Performance of Drilled Piers in Weak Rock. *Canadian Geotechnical Journal*, Vol. 20, No. 4, pp. 758-772.

Ladanyi, B. and Roy, A. (1971). Some Aspects of Bearing Capacity of Rock Mass. Proc., *7th Canadian Symposium on Rock Mechanics*, Edmonton, pp. 161-190.

LOADTEST (2017a). *Report on Bored Pile Load Testing (Osterberg Method), Davies P-15 (sic – STP1) - TransEd Valley Line LRT, Edmonton, AB (LT-1708-1) –* (Document No. 26076-VEN-CP00-00040), January 17, 2017.

LOADTEST (2017b). *Report on Bored Pile Load Testing (Osterberg Method), Davies STP-2 – TransEd Valley Line LRT, Edmonton, AB (LT-1708-2) –* (Document No. 26076-VEN-CP00-00136), April 24, 2017.

LOADTEST (2017c). *Report on Bored Pile Load Testing (Osterberg Method), SRV P-4 (STP-3 adjacent to P-4) - TransEd Valley Line LRT, Edmonton, AB (LT-1708-3)*, January 17, 2017.

Matheson, D.S. (1970). A tunnel roof failure in till. *Canadian Geotechnical Journal,* 7(3), pp. 313-317

Reese, L.C. and O'Neill, M.W. (1987). Drilled Shafts: Construction Procedures and Design Methods. U.S. Department of Transportation.

Rowe, R.K. and Armitage, H.H. (1984). The Design of Piles Socketed into Weak Rock*. Research Report GEOT-11-84,* Faculty of Engineering. Science, University of Western Ontario, London, Ont.

Rowe, R.K. and Armitage, H.H. (1987). A Design Method for Drilled Piers in Soft Rock. *Canadian Geotechnical Journal*, Vol. 24, pp. 126-142.

Ruban, T. and Kort, D. (2011). Pile Load Testing of Concrete Belled Pile and Rock Socket Pile Using the Osterberg Load Cell, *Pan-Am CGS Geotechnical Conference*, Canadian Geotechnical Society, Toronto, Ontario, 8p.

Skinner, G.D., Becker, D.E., and Appleton, B.J.A. (2008). Full-scale Pile Load Testing of Cast-in-Place Caissons using Osterberg Load-Cell Method – Anthony Henday Drive Southeast Ring Road Case Study, Proceedings, *GeoEdmonton 2008*, Canadian Geotechnical Society, 7p.

Stas, C.V and Kulhawy, F.H. (1984). Critical Evaluation of Design Methods for Foundations Under Axial Uplift and Compression Loading. *Report EL-3771,* Electric Power Research Institute, Palo Alto, Calif.

Thompson, S. (1981). Evaluation of Pile Load Tests in the Edmonton Area, *Canadian Journal of Geotechnical Engineering*, Vol. 18, pp. 313-316.

Wang, X., Tweedie, R., and Law, D. (2017). Edmonton ICE District Towers Geotechnical Investigation and Foundation Design, *GeoOttawa 2017*, Canadian Geotechnical Society, 8p.

Weltman, A.J. and Healy, P.R. (1978). *Piling in Boulder Clay and Other Glacial Tills*. Construction Industry Research & Information Association, 78 p.

Williams, A.F., Donald I.B. and Chiu, H.K. (1980). Stress Distributions in Rock Socketed Piles. Proceedings of *the International Conference on Structural Foundations on Rock*, Sydney Australia, pp. 317-326.